JPL Publication D-94649

ECOsystem Spaceborne Thermal Radiometer Experiment on Space Station (ECOSTRESS)

Level-4 Water Use Efficiency L4(WUE) Algorithm Theoretical Basis Document

Joshua B. Fisher, ECOSTRESS Science Lead
ECOSTRESS Algorithm Development Team
ECOSTRESS Science Team
Jet Propulsion Laboratory
California Institute of Technology

May 2018
ECOSTRESS Science Document no. D-94649

**National Aeronautics and
Space Administration**

**Jet Propulsion Laboratory
California Institute of Technology
Pasadena, California**

This research was carried out at the Jet Propulsion Laboratory, California Institute of Technology, under a contract with the National Aeronautics and Space Administration.

Contacts

Readers seeking additional information about this document may contact the following ECOSTRESS Science Team members:

- Joshua B. Fisher
  MS 233-305C
  Jet Propulsion Laboratory
  4800 Oak Grove Dr.
  Pasadena, CA 91109
  Email: jbfisher@jpl.nasa.gov
  Office: (818) 354-0934

- Simon J. Hook
  MS 183-501
  Jet Propulsion Laboratory
  4800 Oak Grove Dr.
  Pasadena, CA 91109
  Email: simon.j.hook@jpl.nasa.gov
  Office: (818) 354-0974
  Fax: (818) 354-5148

List of Acronyms

ATBD	Algorithm Theoretical Basis Document
CONUS	Contiguous United States
ECOSTRESS	ECOsystem Spaceborne Thermal Radiometer Experiment on Space Station
ET	Evapotranspiration
GPP	Gross Primary Production
HyspIRI	Hyperspectral Infrared Imager
ISS	International Space Station
L-3	Level 3
L-4	Level 4
MODIS	MODerate-resolution Imaging Spectroradiometer
OCO	Orbiting Carbon Observatory
PHyTIR	Prototype HyspIRI Thermal Infrared Radiometer
PT-JPL	Priestley-Taylor Jet Propulsion Laboratory
SDS	Science Data System
SIF	Solar induced chlorophyll fluorescence
SMAP	Soil Moisture Active Passive
VIIRS	Visible Infrared Imaging Radiometer Suite
WUE	Water Use Efficiency

Contents

1 Introduction

1.1 Purpose

Plants and ecosystems have highly disparate water consumption (i.e., evapotranspiration, *ET*) needs based on their evolutionary histories, local plasticity and adaptations. Some plants are more efficient with their water use than others, subsequently fixing relatively greater amounts of carbon (C) through photosynthesis (gross primary production, *GPP*) per unit of water lost through ET. This C gain relative to water lost is termed the Water Use Efficiency (*WUE*) [*Stanhill*, 1986; *Stewart and Steiner*, 1990; *Steduto*, 1996]. During times of water shortage or drought, less water use efficient plants may be more vulnerable to stress or mortality than are plants with higher *WUE* [*Keenan et al.*, 2013]. Knowing what and where the *WUE* is of different plants and ecosystems will advance the understanding of how the terrestrial biosphere is responding to changes in climate. A relatively high spatial resolution is necessary to capture *WUE* differences in ecosystems with diverse species assemblages.

ECOSTRESS will be producing *ET* over the entire ECOSTRESS domain as a Level-3 product, L3(ET_PT-JPL) [*Fisher and ECOSTRESS Algorithm Development Team*, 2015]. To generate *WUE* the L4(WUE) product must ingest an ancillary *GPP* product to combine with the L3 *ET* product concurrently measured/produced during the L3 *ET* ECOSTRESS production.

In this Algorithm Theoretical Basis Document (ATBD), we describe the calculation of *WUE* and the ingestion of the *GPP* product. The theoretical basis for the ECOSTRESS *ET* is described in the ECOSTRESS L3(ET_PT-JPL) ATBD. The ECOSTRESS L4(WUE) product is a value-added product to ECOSTRESS.

1.2 Scope and Objectives

In this ATBD, we provide:

1. Description of the general form of the *WUE* equation;
2. Description of the *GPP* ancillary data ingestion.

2 Parameter Description and Requirements

Attributes of the *WUE* data required by the ECOSTRESS mission include:

- Spatial resolution of 70 m x 70 m;
- Latency as required by the ECOSTRESS Science Data System (SDS) processing system;
- Includes all geographic terrestrial regions visible by the ECOSTRESS instrument (i.e., the Prototype HyspIRI Thermal Infrared Radiometer; PHyTIR) from the ISS, with priorities to the ECOSTRESS Science Objective 1 Water Use Efficiency (WUE) target regions ("hotspots"), the ECOSTRESS Science Objective 3 agricultural regions (e.g., the Contiguous United States; CONUS), and the Cal/Val sites (Figure 1).

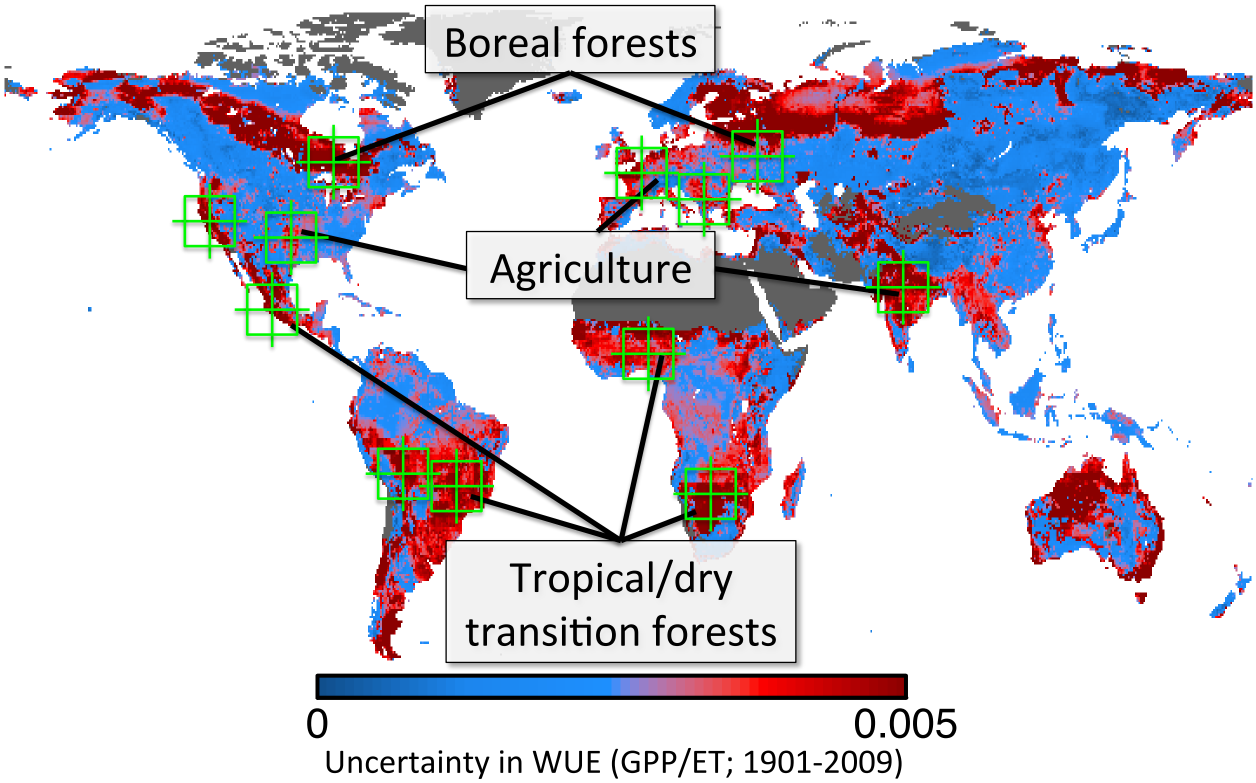

Figure 1. Uncertainty in Water Use Efficiency (WUE) from global models is highlighted in the red areas ("hotspots"). ECOSTRESS will target these regions.

3 Algorithm Selection

The *WUE* algorithm must satisfy basic criteria to be applicable for the ECOSTRESS mission:

- Physically defensible;
- Globally applicable;
- High sensitivity and dependency on remote sensing measurements;
- Relative simplicity necessary for high volume processing;
- Demonstrated sensitivity to vegetation drought conditions;
- Published record of algorithm maturity, stability, and validation.

4 Water Use Efficiency Retrieval

4.1 *Water Use Efficiency (WUE)*

WUE is defined as the ratio of the amount of C fixed in units of GPP (g C m^{-2} d^{-1}) per amount of water lost in units of ET (kg H_2O m^{-2} d^{-1}), which reduces to a daily ratio (g C kg^{-1} H_2O):

$$WUE = \frac{GPP}{ET} \tag{1}$$

High values indicate efficient plants, and low values indicate inefficient plants. The theoretical basis and algorithmic procedures for producing *ET* are described in the ECOSTRESS L3(ET_PT-JPL) ATBD [*Fisher and ECOSTRESS Algorithm Development Team*, 2015].

4.2 *Gross Primary Production (GPP)*

The *GPP* ancillary product may be ingested from any number of sources: MODIS [*Zhao et al.*, 2005], SMAP [*Kimball et al.*, 2014], OCO-2 [*Frankenberg et al.*, 2011; *Frankenberg et al.*, 2014], VIIRS, and OCO-3 [*Eldering et al.*, 2015]. The MODIS product is ideal for ECOSTRESS because it aligns with the other MODIS ancillary products already being ingested into the L3(ET_PT-JPL) algorithm/product, it is given at relatively high spatial and temporal resolutions (1 km, 8-day), and has been vetted in the scientific literature [*Heinsch et al.*, 2006; *Turner et al.*, 2006; *Zhang et al.*, 2012] (Figure 2). VIIRS is expected to mirror many of the major MODIS products, including the GPP product [*Dungan et al.*, 2014]. SMAP now provides a high quality *GPP* product as part of the SMAP L4 carbon product with good temporal resolution and moderate spatial resolution, largely based on MODIS measurements [*Kimball et al.*, 2014] (Figure 3). OCO-2 provides a key

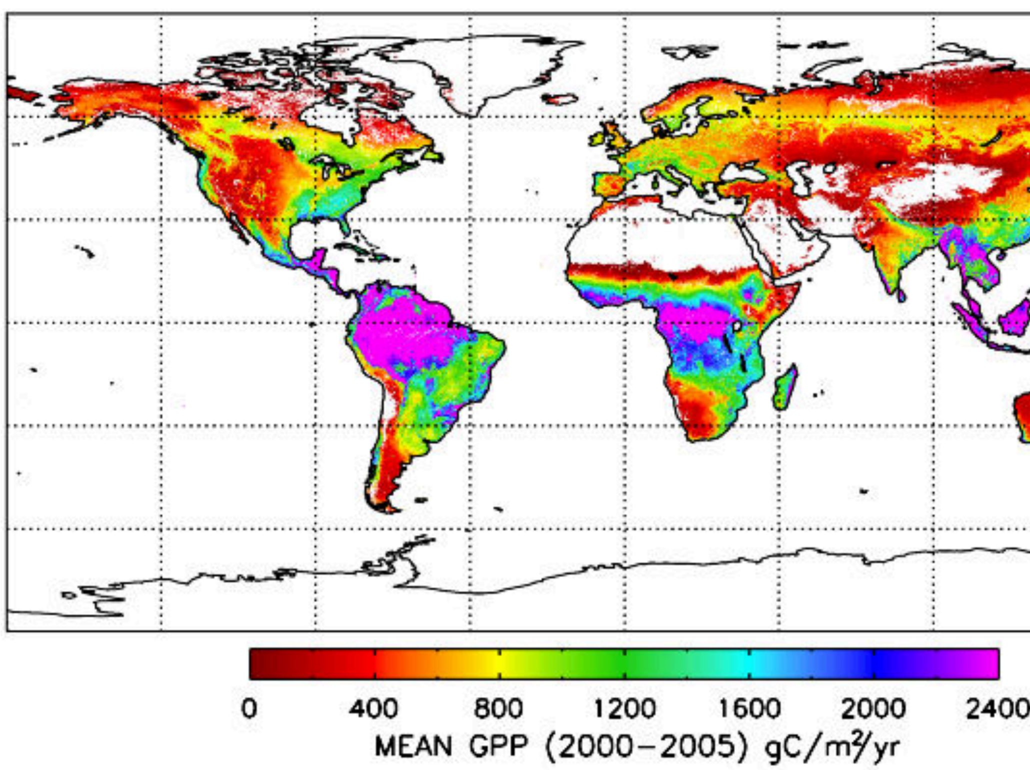

Figure 2. Gross Primary Production (GPP) from MODIS. [*Zhao et al.*, 2005]

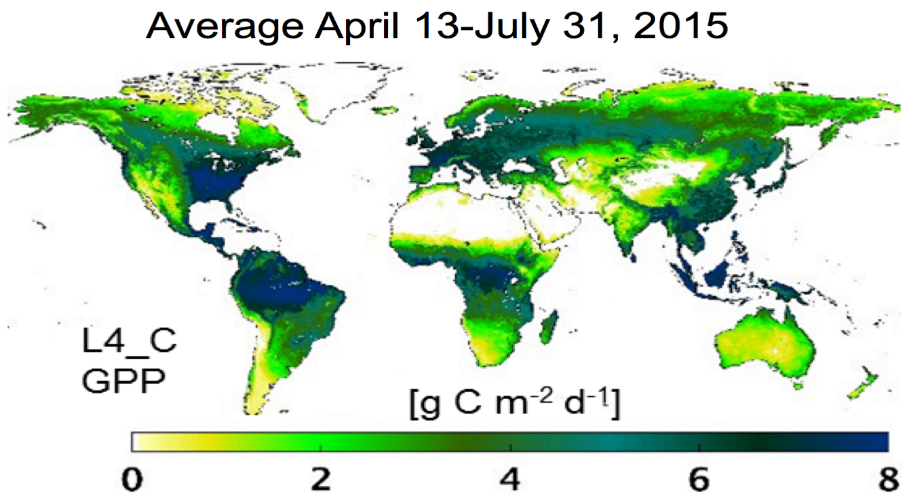

Figure 3. Gross Primary Production (GPP) from the SMAP L4_C product. [*Kimball et al.*, 2014]

measurement—solar induced chlorophyll fluorescence (SIF)—which gives an advancement over MODIS and VIIRS-based GPP estimates, though at coarser resolutions, and which ECOSTRESS Science Lead, Fisher, has already been working with for GPP estimation (Figure 4). Finally, OCO-3, like OCO-2, will provide the same key SIF measurement, and will be on the ISS with ECOSTRESS thereby providing the same orbital characteristics as ECOSTRESS. Nonetheless, it is likely that ECOSTRESS will be on the ISS prior to OCO-3, thus *WUE* would not be able to be produced with OCO-3 until that occurs, so this option is not viable unless the order is switched. The L4(WUE) algorithm is adapted to handle both the MODIS *GPP* and OCO-2 SIF-based *GPP* inputs, with MODIS being the top priority due to its spatial resolution.

The *GPP* product will be ingested operationally into the JPL L3/L4 team's data production stream, divided by the L3(ET_PT-JPL) product, and supplied as *WUE* back to the SDS for delivery to the DAAC according to the ECOSTRESS data delivery schedule. An example of the ECOSTRESS *WUE* simulated from VIIRS LST with MODIS GPP for a single day is given in Figure 5. The accuracy of the *WUE* is dependent on the accuracies of the L3(ET_PT-JPL) and *GPP* products. Higher accuracies and precisions enable small detection differences between ecosystems.

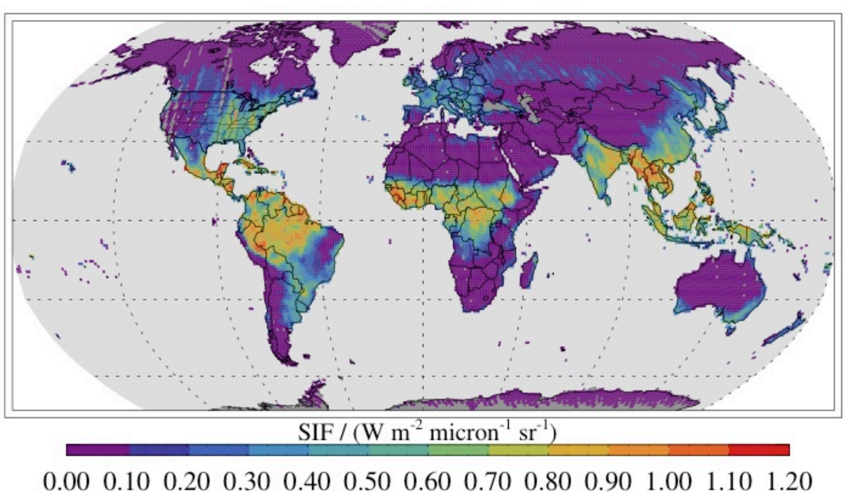

Figure 4. Solar induced chlorophyll fluorescence (SIF) from OCO-2 is linearly proportional to Gross Primary Production (GPP) [*Frankenberg et al.*, 2011; *Frankenberg et al.*, 2014].

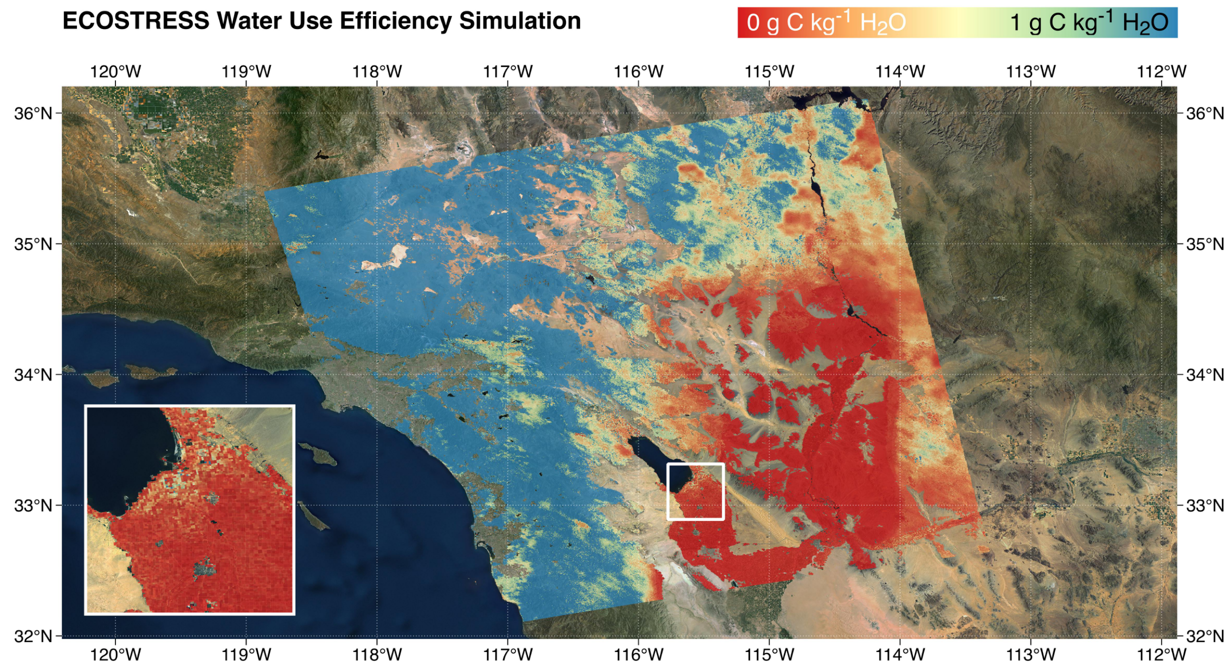

Figure 5. ECOSTRESS WUE (GPP/ET) simulated from VIIRS LST with MODIS GPP for a single day shows regions of low water use efficiency (red) and high water use efficiency (blues).

4.2.1 Diurnal cycling

Except for OCO-3, all the *GPP* options derive from polar orbiters with consistent overpass times, unlike the precessing orbit of ECOSTRESS on the ISS. Thus, the *GPP* product must be statistically shifted to the overpass time of ECOSTRESS for the given day. What is traditionally done, generally, is to construct a date and latitudinal-varying sinusoidal curve mimicking the sunrise-to-sunset radiation intensity [*Bisht et al.*, 2005]. The relative ratios of the instantaneously observed variables (e.g., the *GPP*-to-R_n ratio) are assumed to be held constant throughout that curve/day. Additional refinement may be invoked to include the probabilistic or observed fraction of cloud cover throughout the day and seasonally, land cover or vegetation type-specific parameterizations, and/or dynamically changing relative ratios of the variables of interest.

Because R_n is a major driver of *GPP*, we initialize the diurnal cycle calculation with R_n. *Lagouarde and Brunet* [1993] first developed the framework to obtain the diurnal cycle of T_s from a sinusoidal function with the day length and amplitude equal to the difference between maximum T_s and minimum T_a. *Bisht et al.* [2005] later adapted that to clear sky R_n diurnal cycling:

$$R_n(t) = R_{n,max} sin\left(\pi\left(\frac{t - t_{rise}}{t_{set} - t_{rise}}\right)\right) \tag{9}$$

where $R_{n,max}$ is the maximum value of R_n observed during the given day, and t_{rise} and t_{set} are the local times at which R_n becomes positive and negative, respectively.

The corresponding $R_{n,max}$ for the time of overpass ($t_{overpass}$) is given as:

$$R_{n,max} = \frac{R_{n,overpass}}{sin\left(\pi\left(\frac{t_{overpass}-t_{rise}}{t_{set}-t_{rise}}\right)\right)} \tag{10}$$

The daily average R_n is given as:

$$R_{n,daily} = \frac{\int_{t_{rise}}^{t_{set}} R_n(t)dt}{\int_{t_{rise}}^{t_{set}} dt} = \frac{2R_{n,max}}{\pi} = \frac{2R_{n,overpass}}{\pi sin\left(\pi\left(\frac{t_{overpass}-t_{rise}}{t_{set}-t_{rise}}\right)\right)} \tag{11}$$

The daily-to-instantaneous R_n ratio is therefore:

$$\frac{R_{n,daily}}{R_{n,overpass}} = \frac{2}{\pi sin\left(\pi\left(\frac{T-2a}{2T}\right)\right)} \tag{12}$$

where T is day length (i.e., t_{set} minus t_{rise}), and a is the difference in time between when R_n is maximum and when the satellite overpasses.

For ECOSTRESS, the general form of this equation is applied every day to each of the diurnally-varying R_n drivers (excluding solar zenith angle and T_s and ε_S, the latter two of which are measured at diurnally-varying times of day directly from ECOSTRESS), but the modified instantaneous values are extracted from the equation rather than the daily average.
Issues of extrapolation into cloud cover are circumvented because ECOSTRESS will produce *ET* only under clear-sky conditions; similarly, ECOSTRESS will not produce *WUE* if *GPP* is unavailable due to cloud cover.

4.2.2 Spatial resolution improvements

The L3(ET_PT-JPL) ECOSTRESS product will be given at 70 m x 70 m spatial resolution (though with caveats—see, L3(ET_PT-JPL) ATBD). The *GPP* product will be provided at a spatial resolution coarser than ECOSTRESS, e.g., 1 km x 1 km from MODIS. The *GPP* product will be sub-sampled to match the 70 m x 70 m ECOSTRESS spatial resolution both for consistency as well as use of the high resolution of the *ET* product; however, we caution analyses of *WUE* at <1 km as the "true" resolution will be somewhere between 70 m and 1 km, depending on the relative sensitivity of *WUE* to *ET* for any given place and time, as well as the relative sub-pixel homogeneity/heterogeneity of the *GPP* pixel.

5 Mask/Flag Derivation

The L3(ET_PT-JPL) quality flags are carried over identically to L4(WUE). No additional quality flags are incorporated from those provided by the ancillary *GPP* product (Table 1):

Table 1. ECOSTRESS L4(WUE) MODIS ancillary data flags and responses to poor quality.

Input product	Quality Flag	Response to poor quality
MODIS GPP	N/A	N/A

6 Metadata

- unit of measurement: units of *GPP* per units of *ET* (g C kg^{-1} H_2O)
- range of measurement: 0 to 10
- projection: ECOSTRESS swath
- spatial resolution: 70 m x 70 m
- temporal resolution: dynamically varying with precessing ISS overpass; instantaneous throughout the day, local time
- spatial extent: all land globally, excluding poleward ±60°
- start date time: near real-time
- end data time: near real-time
- number of bands: not applicable
- data type: float
- min value: 0
- max value: 3000
- no data value: 9999
- bad data values: 9999
- flags: quality level 1-4 (best to worst)

7 Acknowledgements

We thank Gregory Halverson, Laura Jewell, and Gregory Moore for contributions to the algorithm development described in this ATBD.

8 References

Bisht, G., V. Venturini, S. Islam, and L. Jiang (2005), Estimation of the net radiation using MODIS (Moderate Resolution Imaging Spectroradiometer), *Remote Sensing of Environment*, *97*, 52-67.

Dungan, J., S. Ganguly, F. Melton, J. Shupe, and R. Nemani (2014), Preliminary vegetation index products from Suomi NPP VIIRS illuminate the California drought, paper presented at AGU Fall Meeting Abstracts.

Eldering, A., R. Basilio, and M. Bennett (2015), The OCO-3 Mission: Overview of Science Objectives and Status, in *American Geophysical Union Fall Meeting*, edited, San Francisco.

Fisher, J. B., and ECOSTRESS Algorithm Development Team (2015), ECOsystem Spaceborne Thermal Radiometer Experiment on Space Station (ECOSTRESS): Level-3 Evapotranspiration Algorithm Theoretical Basis Document*Rep.*, 24 pp, Jet Propulsion Laboratory, Pasadena.

Fisher, J. B., G. J. Moore, and M. K. Verma (2015), Net Radiation and Evapotranspiration (Rn/ET) Download Product Tools and Interfaces, in *NASA Tech Briefs*, edited, NASA.

Frankenberg, C., C. O'Dell, J. Berry, L. Guanter, J. Joiner, P. Köhler, R. Pollock, and T. E. Taylor (2014), Prospects for chlorophyll fluorescence remote sensing from the Orbiting Carbon Observatory-2, *Remote Sensing of Environment*, *147*, 1-12.

Frankenberg, C., J. B. Fisher, J. Worden, G. Badgley, S. S. Saatchi, J.-E. Lee, G. C. Toon, A. Butz, A. Kuze, and T. Yokota (2011), New global observations of the terrestrial carbon cycle from GOSAT: Patterns of plant fluorescence with gross primary productivity, *Geophysical Research Letters*, *38*(L17706), doi:10.1029/2011GL048738.

Heinsch, F. A., M. S. Zhao, S. W. Running, J. S. Kimball, R. R. Nemani, K. J. Davis, P. V. Bolstad, B. D. Cook, A. R. Desai, D. M. Ricciuto, B. E. Law, W. C. Oechel, H. Kwon, H. Luo, S. C. Wofsy, A. L. Dunn, J. W. Munger, D. D. Baldocchi, L. Xu, D. Y. Hollinger, A. D. Richardson, P. C. Stoy, M. B. S. Siqueira, R. K. Monson, S. P. Burns, and L. B. Flanagan (2006), Evaluation of remote sensing based terrestrial productivity from MODIS using regional tower eddy flux network observations, *IEEE Transactions on Geoscience and Remote Sensing*, *44*, 1908-1925.

Keenan, T. F., D. Y. Hollinger, G. Bohrer, D. Dragoni, J. W. Munger, H. P. Schmid, and A. D. Richardson (2013), Increase in forest water-use efficiency as atmospheric carbon dioxide concentrations rise, *Nature*, *499*(7458), 324-327.

Kimball, J. S., L. A. Jones, J. P. Glassy, and R. Reichle (2014), SMAP Level 4 Carbon Data Product (L4_C).

Lagouarde, J., and Y. Brunet (1993), A simple model for estimating the daily upward longwave surface radiation flux from NOAA-AVHRR data, *International Journal of Remote Sensing*, *14*(5), 907-925.

Moore, G. (2015), Rn/ET Download Product Tools and Interfaces*Rep.*, Jet Propulsion Laboratory, California Institute of Technology, Pasadena.

Stanhill, G. (1986), Water Use Efficiency, in *Advances in Agronomy*, edited by N. C. Brady, pp. 53-85, Academic Press.

Steduto, P. (1996), Water use efficiency, in *Sustainability of Irrigated Agriculture*, edited, pp. 193-209, Springer.

Stewart, B., and J. Steiner (1990), Water-use efficiency, in *Advances in soil science*, edited, pp. 151-173, Springer.

Turner, D. P., W. D. Ritts, W. B. Cohen, S. T. Gower, S. W. Running, M. Zhao, M. H. Costa, A. A. Kirschbaum, J. M. Ham, S. R. Saleska, and D. E. Ahl (2006), Evaluation of MODIS NPP and GPP products across multiple biomes, *Remote Sensing of Environment*, *102*(3-4), 282-292.

Zhang, F., J. M. Chen, J. Chen, C. M. Gough, T. A. Martin, and D. Dragoni (2012), Evaluating spatial and temporal patterns of MODIS GPP over the conterminous US against flux measurements and a process model, *Remote Sensing of Environment*, *124*, 717-729.

Zhao, M. S., F. A. Heinsch, R. R. Nemani, and S. W. Running (2005), Improvements of the MODIS terrestrial gross and net primary production global data set, *Remote Sensing of Environment*, *98*, 164-176.